Non-linear Registration Between 3D Images Including Rigid Objects: Application to CT and PET Lung Images With Tumors

A. Moreno[1,2] G. Delso[3] O. Camara[4] I. Bloch[1]

Antonio.Moreno@enst.fr

[1] GET-ENST, Dept. TSI, CNRS UMR 5141 LTCI, Paris, France
[2] Segami Corporation, Paris, France [3] Philips Medical Systems, Suresnes, France
[4] Center for Medical Image Computing, University College London, UK

Abstract

This paper deals with the problem of non linear image registration is the case the images include objects undergoing different types of deformation. As an illustrative application, we consider the registration of CT and PET images of thoracic and abdominal regions. Registration of these two modalities has to cope with deformations of the lungs during breathing. Potential tumors in the lungs usually do not follow the same deformations, since they can be considered as almost rigid, and this should be taken into account in the registration procedure. We show in this paper how to introduce rigidity constraints into a non-linear registration method. The proposed approach is based on registration of landmarks defined on the surface of previously segmented objects and on continuity constraints. The results demonstrate a significant improvement of the combination of anatomical and functional images for diagnosis and for oncology applications.

1 Introduction

Registration between several images of the same scene is a widely addressed topic and is important in many different domains. One of the difficult problems concerns the case where the images include objects undergoing different types of deformation that have to be compensated during the registration. In particular, the behavior of the registration close to the interfaces between such objects has to be carefully controlled in order to avoid discontinuities or other unrealistic phenomena. The aim of this paper is to address this problem.

As an illustrative application, we consider Computed Tomography (CT) and Positron Emission Tomography (PET) in thoracic and abdominal regions, which furnish complementary information about the anatomy and the metabolism of human body. Their combination has a significant impact on improving medical decisions for diagnosis and therapy [16] even with combined PET/CT devices where registration remains necessary to compensate patient respiration and heart beating [14]. Registration of these two modalities is

a challenging application due to the poor quality of the PET image and the large deformations involved in these regions.

Most of the existing methods have as a limitation that regions placed inside or near the main structures will be deformed more or less according to the registration computed for the latter, depending on how local is the deformation. A critical example of this situation occurs when a tumor is located inside the lungs and there is a large volume difference between CT and PET images (due to the breathing). In this case, if the tumor is registered according to the transformation computed for the lungs, it may take absurd shapes, such as shown in Figure 1.

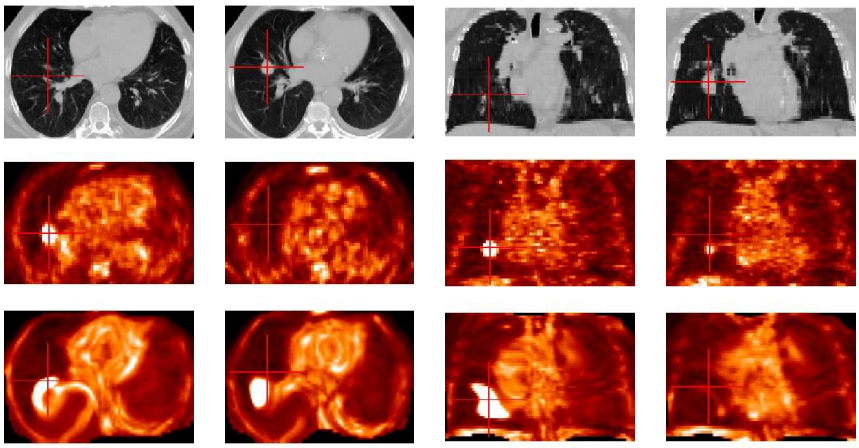

Figure 1: Axial and coronal slices in CT (first row) and in PET (second row). Result of the non-linear registration without tumor-based constraints (third row). The absence of these constraints leads to undesired and irrelevant deformations of the pathology. On the images of the first and third columns, the cursor is positioned on the tumor localization in PET data, while in the second and fourth columns, it is positioned on the tumor localization in CT data. This example shows an erroneous positioning of the tumor and illustrates the importance of the use of tumor-specific constraints.

In this case, two very different deformations exist: the non-linear deformations of the lungs due to the breathing and the linear displacement of the tumor during the breathing cycle. Thus, the aim of this paper is to avoid the undesired tumor misregistrations by adding some rigidity constraints on the tumors. The goal is to preserve tumor geometry and, in particular, intensity since it is critical for clinical studies, for instance based on SUV (Standardized Uptake Value) [6], and for diagnosis and radiotherapy planning.

In Section 2, we summarize existing work related to this subject and we provide an overview of the proposed approach. The introduction of tumor-based constraints into the registration algorithm is detailed in Section 3. Section 4 presents some results obtained on real data. Finally, conclusions and future works are discussed in Section 5.

2 Related Work and Overview of the Proposed Approach

Some approaches have already been developed for registration of multimodality images in pathological cases (pulmonary nodules, cancer), such as in [2]. However these approaches compute a rigid (or affine) registration for all the structures and they do not take into account the local nature of the deformations.

Tanner et al. [15] have developed a method of non-rigid registration based on B-spline Free-Form Deformations (FFD) as in [3]. Their algorithm is applied on MR breast images and it guarantees volume and shape preservation in the rigid regions defined by the lesions. However, the region of the rigid transformation is larger than the lesions. Another approach that uses B-spline FFD is the one by Rohlfing and Maurer [12]. They have used a grid refinement and added some incompressibility constraints (using the properties of the Jacobian) which only guarantee the preservation of the volume of the structures but not their shape. Loeckx et al. [10] have added a local rigidity constraint in order to guarantee shape preservation and they have obtained very promising results. Nevertheless, this algorithm does not enforce the considered structures to be totally rigid, therefore they actually might be slightly deformed.

The recent work of Hachama et al. [7] uses a Bayesian framework in order to characterize the pathologies as outliers of a probabilistic distribution. Their method is applied to mammogram registration and proved to be robust. An implicit assumption is that grey levels in both images are similar, thus making the method appropriate for mono-modality images. This assumption should be relaxed to extend the method to multimodality images.

A different approach, that we consider closer to physical reality of human body, is based on the combination of rigid and non-rigid deformations, as suggested by Little et al. [9] and Huesman et al. [8]. These methods are based on the use of point interpolation techniques, together with a weighting of the deformation according to a distance function. Castellanos et al. [4] developed a slightly different methodology, in which local non-rigid warpings are used to guarantee the continuity of the transformation.

The advantage of these approaches is that they take into account rigid structures and the deformations applied to the image are continuous and smooth. The method we propose is inspired by these ones and adapted to develop a registration algorithm for the thoracic region in the presence of pathologies. In order to illustrate our algorithm, we have applied it on medical data. These data consist of 3D CT and PET images of pathological cases, exhibiting tumors in the lungs. We assume that the tumor is rigid and thus a linear transformation is sufficient to cope with its movements between CT and PET images. This hypothesis is relevant and in accordance with the clinicians' point of view, since tumors are often a compact mass of pathological tissue. In order to guarantee a good registration of both normal and pathological structures, the first step consists of a segmentation of all structures which are visible in both modalities. Then we define two groups of landmarks in both images, which correspond to homologous points, and will guide the deformation of the PET image towards the CT image. The positions of the landmarks are therefore adapted to anatomical shapes. This is an important feature and one of the originalities of our method. The deformation at each point is computed using an interpolation procedure based on the landmarks, on the specific type of deformation of each landmark depending on the structure it belongs to, and weighted by a distance function, which guarantees that the transformation will be continuous.

Thus, the proposed approach has two main advantages:

1. As the transformation near the tumor is reduced by using the distance weight, even if we have some small errors in the tumor segmentation (often quite challenging, mainly in CT), we will obtain a consistent and robust transformation.

2. In the considered application, one important fact is that the objects to register are not the same in the two images. For instance, the volume of the "anatomical" tumor in CT is not necessarily the same as the volume of the "functional" tumor in PET because the two modalities highlight different characteristics of the objects. The registration of these two views of the tumor must preserve these local differences, which can be very useful because we could discover a part of the anatomy that is touched by the pathology and could not be seen in the CT image. This also advocates in favor of a rigid local registration.

3 Combining Rigid and Non-linear Deformations

Based on a segmentation of the objects visible in both images, pairs of homologous points are defined. They constitute landmarks guiding the registration. We assume that globally a non-linear transformation has to be found, while for some objects $O_1,\ldots,O_{n_0}$ (tumors in our application) specific constraints have to be incorporated. For instance, these objects may undergo only a rigid transformation between both images. The global transformation is then interpolated over the whole image. We introduce the rigid structures constraints so that the non-rigid transformation is gradually weighted down in the proximity of objects $O_1,\ldots,O_{n_0}$.

Point-Based Displacement Interpolation

The first step in a point-based interpolation algorithm concerns the selection of the landmarks guiding the transformation. Homologous structures in both images are then registered based on landmarks defined on their surface. The resulting deformation will be exact at these landmarks and smooth elsewhere, which is achieved by interpolation.

Let us denote by $\mathbf{t}_i$ the n landmarks in the source image that we want to transform to new sites $\mathbf{u}_i$ (the homologous landmarks) in the target image.

The deformation at each point $\mathbf{t}$ in the image is defined as:

$$\mathbf{f}(\mathbf{t}) = \mathscr{L}(\mathbf{t}) + \sum_{j=1}^{n} B_j^T \sigma(\mathbf{t},\mathbf{t}_j) \tag{1}$$

under the constraints

$$\forall i, \quad \mathbf{u}_i = \mathbf{f}(\mathbf{t}_i). \tag{2}$$

The first term, $\mathscr{L}(\mathbf{t})$, represents the linear transformation of every point $\mathbf{t}$ in the source image. When n_0 rigid objects ($O_1,O_2,\ldots,O_{n_0}$) are present, the linear term is a weighted sum of each object's linear transformation. The weights $w_i(\mathbf{t})$ are dependent on a measure of distance $d(\mathbf{t},O_i)$ from the point $\mathbf{t}$ to the object O_i as described in [9]:

$$w_i(\mathbf{t}) = \begin{cases} 1 \text{ if } \mathbf{t} \in O_i \\ 0 \text{ if } \mathbf{t} \in O_j,\ j=1,\ldots,n_0,\ j \neq i \\ \frac{q_i(\mathbf{t})}{\sum_{j=1}^{n_0} q_j(\mathbf{t})} \text{ otherwise} \end{cases} \quad \text{where} \quad q_i(\mathbf{t}) = \frac{1}{d(\mathbf{t},O_i)^{\mu}} \tag{3}$$

and $\mu = 1.5$ (for the work illustrated in this paper).

Therefore, for any point $\mathbf{t}$ we define our linear transformation as:

$$\mathscr{L}(\mathbf{t}) = \sum_{i=1}^{n_0} w_i(\mathbf{t}) L_i \tag{4}$$

where $L_i,\ i = 1,\ldots,n_0$ are the linear transformations of the rigid objects. The closer $\mathbf{t}$ is to the object O_i, the more similar its linear transformation will be to L_i.

The second term represents the non-linear transformation which is, for a point $\mathbf{t}$, the sum of n terms, one for each landmark. Each term is the product of the coefficients of a matrix B (that will be computed in order to satisfy the constraints on the landmarks) with a function $\sigma(\mathbf{t},\mathbf{t}_j)$, depending on the (normalized) distance between $\mathbf{t}$ and $\mathbf{t}_j$:

$$\sigma(\mathbf{t},\mathbf{t}_j) = |\mathbf{t}-\mathbf{t}_j|. \tag{5}$$

This form has favorable properties for image registration [17]. However, different functions could be used, as the one described in [9].

With the constraints given by Equation 2, we can calculate the coefficients B of the non-linear term by expressing Equation 1 for $\mathbf{t} = \mathbf{t}_i$. The transformation can then be defined in a matricial way:

$$\Sigma B + L = U \tag{6}$$

where U is the matrix of the landmarks $\mathbf{u}_i$ in the target image (the constraints), $\Sigma_{ij} = \sigma(\mathbf{t}_i,\mathbf{t}_j)$ (given by Equation 5), B is the matrix of the coefficients of the non-linear term and L represents the application of the linear transformations to the landmarks in the source image, $\mathbf{t}_i$.

From Equation 6, the matrix B is obtained as: $B = \Sigma^{-1}(U-L)$. Once the coefficients of B are found, we can calculate the general interpolation solution for every point in $\mathbb{R}^3$ as shown in Equation 1.

Introducing Rigid Structures

In this section, we show how to introduce the constraints imposed by the rigid structures in the images.

To add the influence of the rigid structures $O_1,\ldots,O_{n_0}$, we have redefined the function $\sigma(\mathbf{t},\mathbf{t}_j)$ as $\sigma'(\mathbf{t},\mathbf{t}_j)$ in the following way:

$$\sigma'(\mathbf{t},\mathbf{t}_j) = d(\mathbf{t},O_0)d(\mathbf{t}_j,O_0)\sigma(\mathbf{t},\mathbf{t}_j) \tag{7}$$

where $d(\mathbf{t},O_0)$ is a measure of the distance from point $\mathbf{t}$ to the union of rigid objects $O_0 = O_1 \cup O_2 \cup \ldots \cup O_{n_0}$. It is equal to zero for $\mathbf{t} \in O_0$ (inside any of the rigid structures) and takes small values when $\mathbf{t}$ is near one of the structures. This measure of the distance is continuous over $\mathbb{R}^3$ and it weights the function $\sigma(\mathbf{t},\mathbf{t}_j)$ (see Equation 5). Thus the importance of the non-linear deformation is controlled by the distance to the rigid objects in the following manner:

- $d(\mathbf{t},O_0)$ makes $\sigma'(\mathbf{t},\mathbf{t}_j)$ tend towards zero when the point for which we are calculating the transformation is close to one of the rigid objects;
- $d(\mathbf{t}_j,O_0)$ makes $\sigma'(\mathbf{t},\mathbf{t}_j)$ tend towards zero when the landmark $\mathbf{t}_j$ is near one of the rigid objects. This means that the landmarks close to the rigid structures hardly contribute to the non-linear transformation computation.

Note that this formalism could be more general by replacing $d(\mathbf{t}, O_0)$ by any function of the distance to O_0 that characterizes accurately the behavior of the surrounding regions. Further research is necessary to define such a function in the case of lung tumors. We have used a linear (normalized) distance function as a first approach.

Finally, Equation 6 is rewritten by replacing Σ by Σ', leading to a new matrix B'. We can then calculate the general interpolation solution for every point in $\mathbb{R}^3$ as in Equation 1.

Definition of landmarks and matching

Landmarks can be defined according to the needs of each specific application. They can be uniformly distributed over the surface of homologous objects or based on points having specific properties (maximum of curvature, points undergoing the largest deformations, etc). In our application, we first define a set of landmarks on the surface of the lungs on the CT image, because it has a much better resolution than the PET image. They are approximately uniformly distributed on the surface. Then, we calculate the corresponding points on the surface of the segmented lungs in PET. This is automatically computed by using the Iterative Closest Point (ICP) algorithm [1] and avoids defining by hand the landmarks on both images.

4 Results

We present in this section some results that we have obtained on synthetic, segmented and real images. The structures and the tumors are segmented using the methods in [5] and then, based on pairs of corresponding landmarks in the CT and the PET images, the transformation is computed over the whole image. As mentioned in Section 2, it is reasonable to assume a rigid transformation between the tumors in CT and in PET. As a first approach, we have used a translation. Each translation L_i, $i = 1, \ldots, n_0$ is directly obtained from the segmentation results.

Synthetic images

This first experiment on synthetic images aims at checking that the rigid structures are transformed rigidly, that the landmarks are correctly translated too and, finally, that the transformation elsewhere is consistent and smooth.

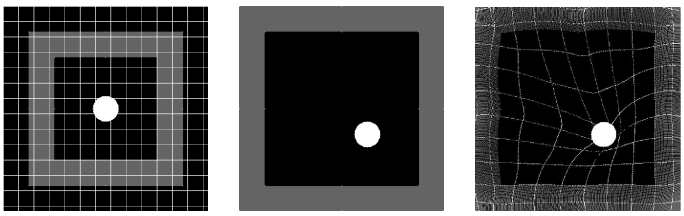

Figure 2: Result on synthetic images: the effect of expanding a frame (in grey in the figure) and translating the "tumor" (in white in the figure). The source image (with a grid) is shown on the left, the target image is in the middle and the result of the transformation on the right. The landmarks are located on the internal and external edges of the frame in grey (on the corners and in the middle of the sides). The total number of landmarks is 16.

As we are taking the PET image as the one to be deformed (source image), we simulate an expansive transformation because the lungs in PET are usually smaller than in

CT images. This is due to the fact that the CT image is often acquired in maximal inspiration of the patient. A simple translation of the "tumor" is simulated too. In order to observe the transformation all over the image, we have plotted a grid on it. It can be seen in Figure 2 that the results with the synthetic images are satisfactory as the shape of the rigid structure (the "tumor") is conserved and the landmarks are translated correctly. The frame, on which the landmarks are placed, is deformed in a continuous and smooth way. If we do not apply the constraints on the rigid structure we obtain an undesired transformation. This is illustrated in [11]. However, it must be noticed that the edges of the frame are not totally straight after the transformation. In general, the more landmarks we have, the better the result will be, and the positions of the landmarks are also very important. Here we have chosen to distribute them uniformly over the internal and external edges of the frame.

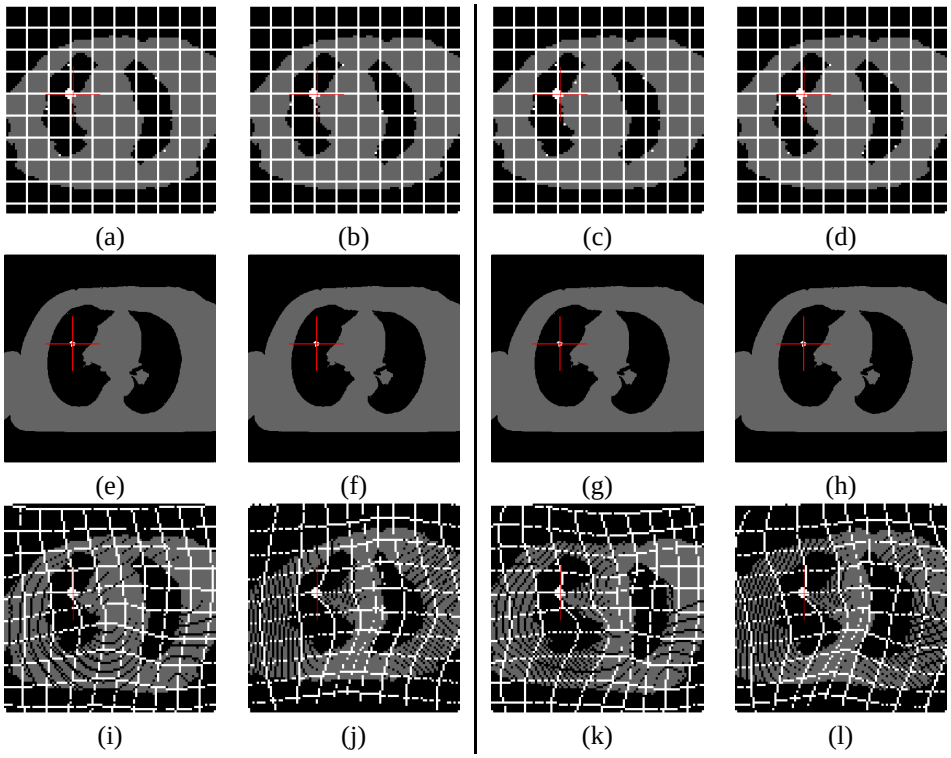

Figure 3: Results on simplified images. Top row: segmented PET images with a grid for visualization purpose (landmarks are also marked in white). Middle row: segmented CT images. Bottom row: results of the registration of the simplified PET and CT images using 4 landmarks (fixed on the corners of the image) and additional landmarks on the walls of the lungs. Left columns: 8 landmarks are chosen on the walls of the lungs using different distributions. Right columns: 12 landmarks are chosen on the walls of the lungs using different distributions. In all the images the cursor is centered on the tumor in the CT image.

Segmented Images

In order to appreciate more clearly the effect of the transformation, we have applied the proposed approach on segmented images. Figure 3 shows some results on the simplified

(segmented) images. A grid is superimposed on the segmented PET image for better visualization. We have fixed the corners of the images to avoid undesired deformations (see illustrations in [11]). It can be observed that for any number of landmarks, the tumor is registered correctly with a rigid transformation. Nevertheless, the quality of the result depends on the quantity of landmarks and their positions. If the number of landmarks is too low or their distribution on the surfaces is not appropriate, the algorithm does not have enough constraints to find the desired transformation. Here the results are obtained by applying the direct transformation in order to better appreciate the influence of the deformation in every region of the image. However it is clear that the final result should be based on the computation of the inverse transformation at each point of the result image in order to avoid unassigned points.

Real Images

Figure 4 shows the results on real images. The tumor is registered correctly with a rigid transformation in all the cases. However, the accuracy of the registration depends on the number and the distribution of the landmarks. If the number of landmarks is not sufficient there are errors. It can be seen that with an appropriate number of landmarks the registration is very satisfactory. The best results (Figure 4(d)) are obtained with 16 landmarks placed as in Figure 3(l). In particular, they include high curvature points. The lower part of the lungs is better registered and the walls of the lungs are perfectly superimposed. The results are considerably improved using 16 landmarks, compared to those obtained with 12 or less landmarks. This shows that the minimal number of landmarks does not need to be very large if the landmarks are correctly distributed.

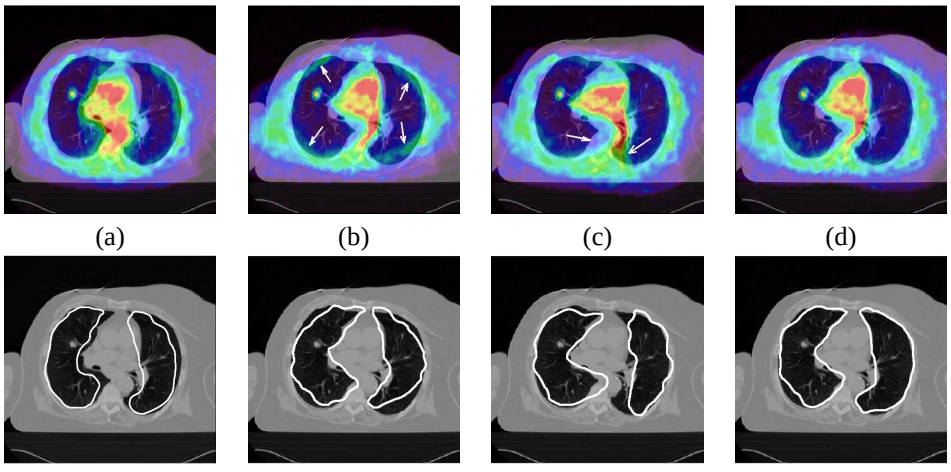

Figure 4: Results on real images. Superimposition of the CT image with: the original PET before registration (a), the deformed PET image using 12 (b) and 16 (c, d) landmarks. (e-h): same results as in (a-d) showing only the contours of the lungs in PET on the CT image. The locations and distribution of the landmarks in (c) are different from the ones in (d) what implies different results. Arrows show misregistrations. This illustrates the importance of the choice of the appropriate landmarks.

5 Conclusion and Future Work

We have developed a non-linear registration method incorporating constraints on deformations of specified objects. It has been shown to be adapted to images which contain rigid structures. The method consists in computing a deformation guided by a group of landmarks and with rigidity constraints. This method has been illustrated on the example of CT/PET registration, in pathological cases where most tissues undergo non-linear transformations due to breathing while tumors remain rigid. In this application, results are very satisfactory and our algorithm avoids undesired tumor misregistrations and preserves tumor geometry and intensity.

One of the originalities of our approach, in particular compared to the method in [9], is that the positions of the landmarks are adapted to the shapes of the structures in the images. In addition to this, with our algorithm, the landmarks are only defined manually in one of the images (the CT) and automatically in the second one (the PET) by means of the ICP algorithm. In the illustrated application, as the transformation near the tumor is reduced by a weight depending on a distance measure, even if the tumor segmentation is not perfect, the registration remains consistent and robust. Moreover, the tumor in CT and PET has not necessarily the same size and shape, therefore the registration of these two modalities is very useful because all the information of the PET image is preserved. This is very important in order to know the true extension of the pathology for diagnosis and for the treatment of the tumor with radiotherapy, for example.

The choice of the landmarks in the CT image is done manually for the moment. However, future work aims at developing an automatic method for defining the landmarks homogeneously distributed all over the surface and on the regions of maximum curvature. A quantitative measure of the alignment between the images will be used in order to find the best distribution of the landmarks that minimizes this similarity measure.

It is also necessary to carry out a detailed study of the rigidity properties of the tissues surrounding a pathology. Replacing the distance by another function would then be straightforward using our formulation.

Although validation is a common difficulty in registration [13], we plan an evaluation phase in collaboration with clinicians, as well as comparison with other methods.

Acknowledgements

The authors would like to thank Liège, Lille, Louisville and Val de Grâce Hospitals for the images and helpful discussions and the members of Segami Corporation for their contribution to this project. This work was partially supported by the French Ministry for Research.

References

[1] P. J. Besl and N. D. McKay. A Method for Registration of 3-D Shapes. *IEEE Transactions on Pattern Analysis and Machine Intelligence*, 14(2):239–256, February 1992.

[2] T. Blaffert and R. Wiemker. Comparison of Different Follow-Up Lung Registration Methods with and without Segmentation. In *Proceedings of SPIE Medical Imaging 2004*, volume 5370, pages 1701–1708, San Diego, California, USA, February 2004.

[3] O. Camara-Rey. *Non-Linear Registration of Thoracic and Abdominal CT and PET Images: Methodology Study and Application in Clinical Routine*. PhD thesis, ENST 2003 E 043, Ecole Nationale Supérieure des Télécommunications (ENST), Paris, France, December 2003.

[4] N. P. Castellanos, P. L. D. Angel, and V. Medina. Nonrigid Medical Image Registration Technique as a Composition of Local Warpings. *Pattern Recognition*, 37:2141–2154, 2004.

[5] G. Delso. *Registro Elástico de Imágenes Médicas Multimodales. Aplicación en Oncología*. PhD thesis, Centre de Recerca en Enginyeria Biomèdica, Universitat Politècnica de Catalunya, Barcelona, Spain, October 2003.

[6] J. Feuardent, M. Soret, O. de Dreuille, H. Foehrenbach, and I. Buvat. Reliability of SUV Estimates in FDG PET as a Function of Acquisition and Processing Protocols. In *Proceedings of the IEEE Nuclear Science Symposium Conference Record*, volume 4, pages 2877–2881, October 2003.

[7] M. Hachama, F. Richard, and A. Desolneux. A Mammogram Registration Technique Dealing With Outliers. In *Proceedings of the IEEE International Symposium on Biomedical Imaging (ISBI'06)*, Arlington, Virginia, USA, April 2006.

[8] R. H. Huesman, G. J. Klein, J. A. Kimdon, C. Kuo, and S. Majumdar. Deformable Registration of Multimodal Data Including Rigid Structures. *IEEE Transactions on Nuclear Science*, 50(3):4S–14S, June 2003.

[9] J. A. Little, D. L. G. Hill, and D. J. Hawkes. Deformations Incorporating Rigid Structures. *Computer Vision and Image Understanding*, 66(2):223–232, May 1997.

[10] D. Loeckx, F. Maes, D. Vandermeulen, and P. Suetens. Nonrigid Image Registration Using Free-Form Deformations with Local Rigidity Constraint. In *Proceedings of MICCAI 2004*, volume LNCS 3216, pages 639–646, Rennes - St-Malo, France, September 2004.

[11] A. Moreno, G. Delso, O. Camara, and I. Bloch. CT and PET Registration Using Deformations Incorporating Tumor-Based Constraints. In *Proceedings of the 10th Iberoamerican Congress on Pattern Recognition (XCIARP)*, volume LNCS 3773, pages 1–12, La Habana, Cuba, nov 2005.

[12] T. Rohlfing and C. R. Maurer. Intensity-Based Non-Rigid Registration Using Adaptive Multilevel Free-Form Deformation with an Incompressibility Constraint. In *Proceedings of MICCAI 2001*, volume LNCS 2208, pages 111–119, Utrecht, The Netherlands, October 2001.

[13] J. A. Schnabel, C. Tanner, A. D. Castellano-Smith, A. Degenhard, M. O. Leach, D. R. Hose, D. L. G. Hill, and D. J. Hawkes. Validation of Nonrigid Image Registration Using Finite-Element Methods: Application to Breast MR Images. *IEEE Transactions on Medical Imaging*, 22(2):238–247, February 2003.

[14] R. Shekhar, V. Walimbe, S. Raja, V. Zagrodsky, M. Kanvinde, G. Wu, and B. Bybel. Automated 3-Dimensional Elastic Registration of Whole-Body PET and CT from Separate or Combined Scanners. *The Journal of Nuclear Medicine*, 46(9):1488–1496, September 2005.

[15] C. Tanner, J. A. Schnabel, D. Chung, M. J. Clarkson, D. Rueckert, D. L. G. Hill, and D. J. Hawkes. Volume and Shape Preservation of Enhancing Lesions When Applying Non-rigid Registration to a Time Series of Contrast Enhancing MR Breast Images. In *Proceedings of MICCAI 2000*, volume LNCS 1935, pages 327–337, Pittsburgh, USA, 2000.

[16] H. N. Wagner. PET and PET/CT: Progress, Rewards, and Challenges. *The Journal of Nuclear Medicine*, 44(7):10N–14N, July 2003.

[17] R. Wiemker, K. Rohr, L. Binder, R. Sprengel, and H. S. Stiehl. Application of Elastic Registration to Imagery from Airbone Scanners. In *XVIII Congress of the International Society for Photogrammetry and Remote Sensing (ISPRS'96)*, volume XXXI-B4, pages 949–954, Vienna, Austria, 1996.